

Electrical Conductivity and Electronic/Ionic Properties of $\text{TiO}_x\text{-CaO-SiO}_2$ Slags at Various Oxygen Potentials and Temperatures



JUN-HAO LIU, GUO-HUA ZHANG, YUE-DONG WU, and KUO-CHIH CHOU

The electrical conductivity of molten slags is an extremely important factor in the design of electric smelting furnaces. As a fundamental study on properties of the TiO_x -bearing slags, the total electrical conductivity and electronic/ionic properties of $\text{TiO}_x\text{-SiO}_2\text{-CaO}$ slags were measured at different oxygen potentials and temperatures using four-electrode method. The experiment results show that for a specific composition, the temperature dependences of ionic, electronic, and total conductivity obey the Arrhenius law. The stepped potential chronoamperometry method was employed for measuring the electronic transference number, which exhibits a strong dependence on oxygen potential, but is unaffected by temperature. The total electrical, electronic, and ionic conductivities present similar increasing trends with increasing the ratio of CO/CO_2 , which is resulted from increasing of Ti^{3+} .

DOI: 10.1007/s11663-015-0499-3

© The Minerals, Metals & Materials Society and ASM International 2015

I. INTRODUCTION

THE electrical conductivity of molten slags plays an important role in understanding the structure of molten slags and operation of the electric smelting furnace. For instance, molten oxide electrolysis (MOE)^[1-7] is a carbon-neutral electrochemical technique to decompose metal oxide directly into liquid metal and oxygen gas upon use of an inert anode. Compared to other technologies, its potential environmental advantage of no greenhouse gas emissions is the most important characteristic. For such electrometallurgy process, the electrical conductivity of molten slags is particularly important. The electrical conductivities of $\text{TiO}_2\text{-BaO}$,^[8] $\text{Fe}_x\text{O-CaO-SiO}_2$,^[9-12] $\text{Fe}_x\text{O-CaO-MgO-SiO}_2$,^[13] $\text{Fe}_x\text{O-CaO-SiO}_2\text{-Al}_2\text{O}_3$,^[14] $\text{Ni}_x\text{O-CaO-SiO}_2$,^[15] and $\text{Ni}_x\text{O-CaO-MgO-SiO}_2$ ^[15] slags had been measured and reported in published literatures. Due to the high melting point of slags and the transfer of charge between the slag and the adsorbed gas species, the data regarding the electronic properties of TiO_x -bearing slags are very limited. The objective of this work was to study the electrical and electronic conductivity of $\text{TiO}_x\text{-CaO-SiO}_2$ slags at various temperatures and oxygen potentials which was controlled by the ratio of CO/CO_2 . These fundamental researches will be used in the modeling and design of electric smelting furnaces.

II. EXPERIMENTS

The compositions of slag samples are shown in Table I. In each group, the mass ratio of CaO/SiO_2 remains constant, but the content of TiO_2 gradually increases. Slag samples were prepared using reagent grade TiO_2 , SiO_2 , and CaCO_3 powders (analytically pure, Sinopharm Chemical Reagent Co., Ltd, China), all of which were calcined at 1273 K (1000 °C) for 10 hours in a muffle furnace to decompose any carbonate and hydroxide before use. Then, about 12 g mixtures were precisely weighed according to the compositions shown in Table I, and mixed in an agate mortar thoroughly.

To accomplish the electrical conductivity measurements, a four-terminal method was employed in this study. The measurement on the electrical conductivity of $\text{TiO}_x\text{-CaO-SiO}_2$ molten slags is extremely difficult because of its high melting point, reactivity, and conductivity. In order to get an accurate electrical conductivity value, it is necessary to exclude the resistances of lead wires and electrodes from the total measured resistance. If the current electrode is used in common for the potential one, the contribution of the interfacial resistance is usually too large to be disregarded. The application of the four-electrode technique can avoid those difficulties. The electrical conductivity of the melts can be obtained by the following equation:

$$\sigma = C/R_x, \quad [1]$$

where C is the cell constant and R_x is the slag melts resistance. Many factors, such as the applied frequency, the volume of melt, the immersion depths of electrodes in the melt, the positions of electrode, and the temperature could affect the measurement accuracy of the cell constant. Those factors were carefully handled in the present study.

JUN-HAO LIU, Doctoral Student, GUO-HUA ZHANG, Associate Professor, YUE-DONG WU, Master Student, and KUO-CHIH CHOU, Professor, are with the State Key Laboratory of Advanced Metallurgy, University of Science and Technology Beijing 100083, China. Contact e-mail: ghzhang_ustb@163.com

Manuscript submitted June 22, 2015.

Article published online November 2, 2015.

The electronic transference numbers were measured using the stepped potential chronoamperometry (SPC) method.^[16,17] Basically, the current response upon

Table I. Composition of Slag Sample (Mass Pct)

TiO ₂	CaO	SiO ₂	C/S
51.1	24.5	24.5	1
22	39	39	1
14.2	42.9	42.9	1
7.5	46	46.5	1

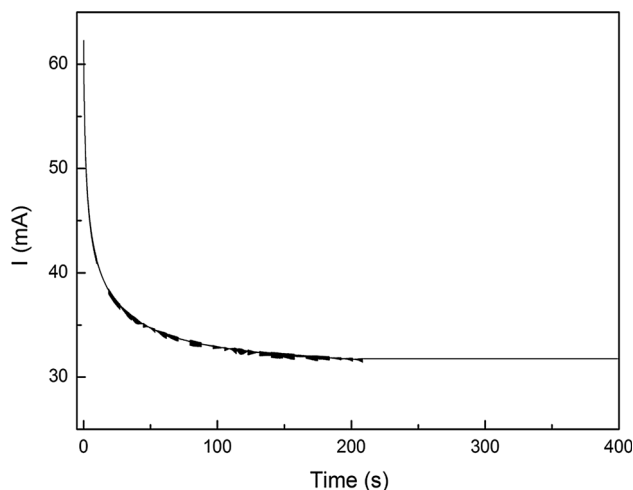


Fig. 1—A typical current vs time curve.

applying a constant voltage (stepped potential) is monitored as a function of time in this technique. The electronic transference number can be calculated using the following equation:

$$t_e = \frac{i_{t \rightarrow \infty}}{i_{t \rightarrow 0}}, \quad [2]$$

where $i_{t \rightarrow 0}$ is the initial value of the current and $i_{t \rightarrow \infty}$ is the long-time value of the current. Figure 1 shows a typical current vs time curve. The experimental arrangement is drawn schematically in Figure 2, and the descriptions of experiment device have already mentioned in our previous study.^[18] The electrodes were made from Pt-Rh (30 wt pct), and each electrode consisted of a tip which is 25-mm long and 0.8-mm in diameter welded to a thinner extension wire which consisted of the same material, but 0.3-mm in diameter and 800-mm long. The electrodes were sheathed into two twin-bore alumina tubes (The distance between two holes is 3 mm) so that the tips were extended about 20 mm outside the tubes. The two twin-bore alumina tubes were fixed with a short alumina tube of the same diameter and these tubes were then passed down two support tubes which were stabilized rigidly, so that these two central electrodes separate for 6 mm. The two twin-bore alumina tubes could be moved up and down along the two support tubes. Before each measurement, the cell calibration for determination of C was performed at low temperatures [293 K to 298 K (20 °C to 25 °C)], using standard aqueous KCl solutions (1.0 mol/L), whose preparation and specific conductance were well documented. The resistance was

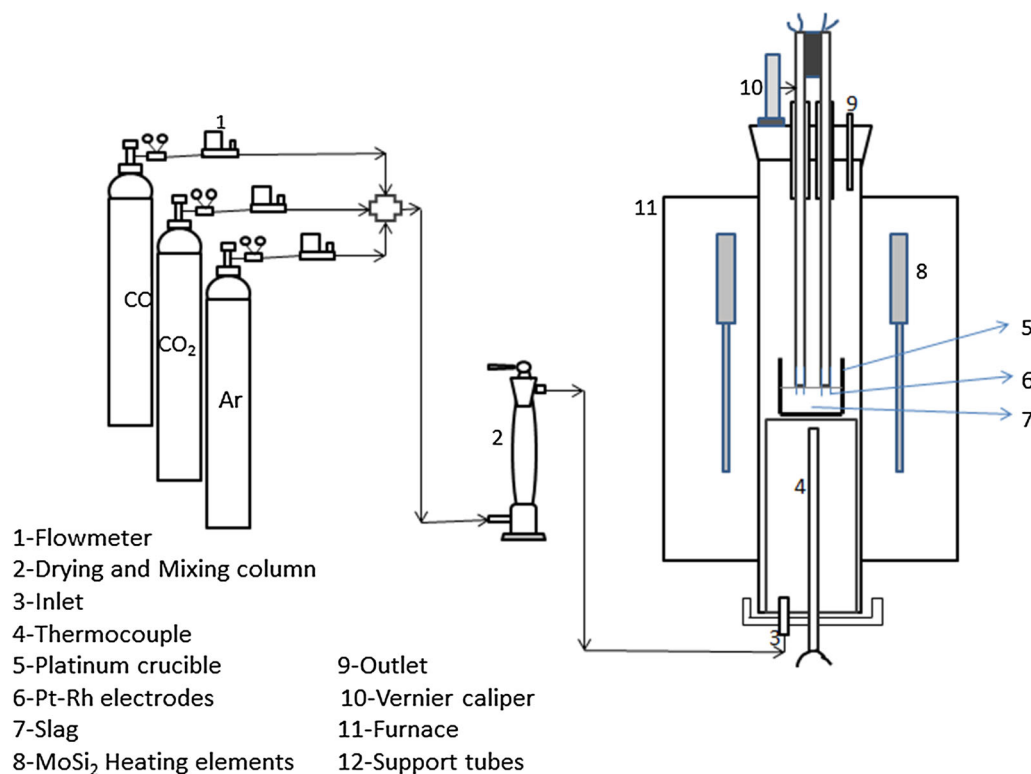


Fig. 2—Schematic diagram of the apparatus.

measured at different immersion depths of the electrodes to determine C by Eq. [1].

After obtaining the cell constant, the prepared slag samples were packed into a platinum crucible (The diameter and height of the crucible are 26 mm and 25 mm, respectively. The depth of the melt is about 12 mm.) and then placed at the constant temperature zone inside the furnace, where the temperature variations measured by a type B (Pt-6 pct Rh/Pt-30 pct Rh) thermocouple could be negligible. During the heating process, the tips of the electrodes were located at about 2 cm above the slag surface. After the target temperature 1843 K (1570 °C) was reached and held for 2 hours, the electrodes were lowered slowly until touched the surface of the melt. During this process, the resistance was monitored. When the tips of the electrodes contacted with the surface of melt, the resistance will significantly decrease, and this position is considered as the zero point. And then the electrodes were lowered further to reach the desired depth. In all experiments, the immersion depth of the electrodes was 3 mm, and the electrodes were in the intermediate position of the crucible during the whole experimental process.

During the whole heating process and the first 2 hours holding at the target temperature, the slag was exposed to CO_2 , and the gas rate was controlled by a flowmeter. The input gas composition varied from pure CO_2 to CO/CO_2 mixed gas to control oxygen partial pressure. The total flow rate of CO_2 and CO was fixed at 200 mL/min. The slag was kept for 2 hours in each atmosphere for the purpose of equilibrium and uniformity of slag. Once the slag and gas reached equilibrium, the electrical measurements were carried out at every 30 K interval on cooling from 1843 K (1570 °C).

The slag resistance was measured using a Model CHI 660a Electrochemical Workstation, and the electronic transference number was measured by the SPC method, using a direct current signal. The resistance was found to be independent of the frequency, over the range 0.5 to 100 kHz. All of the measurements were carried out at 20 kHz.

III. RESULTS AND DISCUSSION

A. Total Electrical Conductivity

1. Influence of oxygen potential on total electrical conductivity

The total electrical conductivity for different compositions at 1843 K (1570 °C) as a function of CO/CO_2 ratio is shown in Figure 3, from which it can be seen that for slags with various TiO_2 contents, the total electrical conductivities increase as increasing the ratio of CO/CO_2 , and the higher the content of TiO_2 is, the higher the total electrical conductivities will be in fixed CO/CO_2 ratio.

2. Influence of temperature on total electrical conductivity

It is widely accepted that the temperature dependence of electrical conductivity can be expressed by the Arrhenius law as

$$\sigma = A \exp(-E/RT) \quad [3]$$

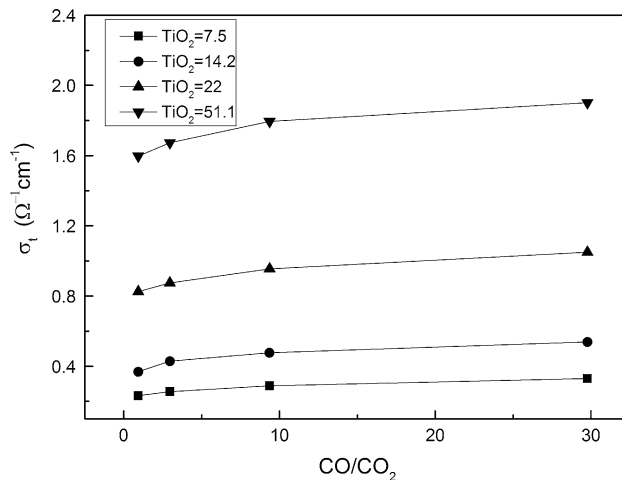


Fig. 3—The total electrical conductivity for different compositions at 1843 K (1570 °C) as a function of CO/CO_2 ratio.

Or

$$\ln \sigma = A \exp(-E/RT), \quad [4]$$

where σ is electrical conductivity, $\Omega^{-1} \text{cm}^{-1}$; A is pre-exponent factor; E is activation energy, $\text{J}/(\text{mol K})$; R is the gas constant, $8.314 \text{ J}/(\text{mol K})$; and T is the absolute temperature, K . Figure 4 shows the change of total electrical conductivity as a function of temperature for different slags, at $\text{CO}/\text{CO}_2 = 30$. It can be seen from Figure 4, electrical conductivity increases as increasing the temperature, furthermore, the temperature dependence of electrical conductivity obeys the Arrhenius law very well, with the activation energies shown in Table II. At the higher temperature, ion mobility will be stronger, which resulted in the increase of electrical conductivity. In addition, temperature will affect the ratio of $\text{Ti}^{3+}/\text{Ti}^{4+}$, which also influences the electrical conductivity of slags.

B. Electronic Transference Number

1. Influence of equilibrium oxygen potential on electronic transference number

The CO/CO_2 dependence of electronic transference number at 1843 K (1570 °C) is shown in Figure 5. It can be seen that the electronic transference numbers vary from about 42 to 52 pct under the experimental conditions. From Figure 5, the electronic transference numbers always increase as increasing of the CO/CO_2 ratio.

2. Influence of temperature on electronic transference number

The effect of temperature on the electronic transference number is shown in Figure 6, from which it can be seen that the electronic transference number increases with increasing TiO_2 content at $\text{CO}/\text{CO}_2 = 30$. It also obviously shows that the electronic transference number is essentially independent of the temperature under the experimental conditions. Similar trends have been reported by other authors.^[19,20]

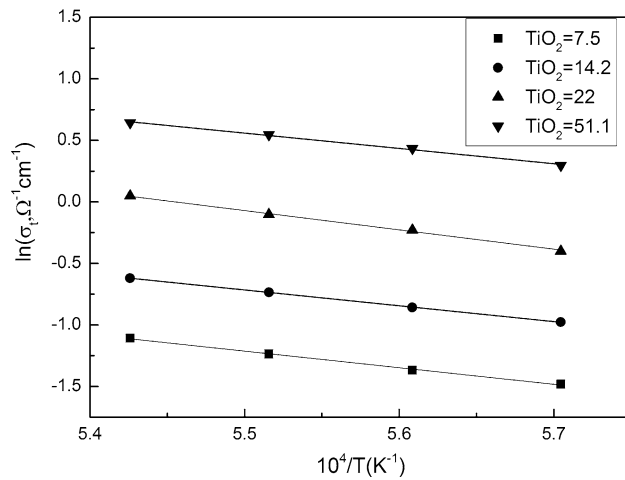


Fig. 4—The change of total electrical conductivity as a function of temperature for different slags, at CO/CO₂ = 30.

Table II. The Activation Energy of Total and Partial Electrical Conductivities, at CO/CO₂ = 30 (kJ/mol)

TiO ₂	7.5	14.2	22	51.1
E (total)	173.3	172.6	162.1	158.3
E (ionic)	172.5	170.8	163.7	158.5
E (electronic)	174.7	171.6	157.8	157.6

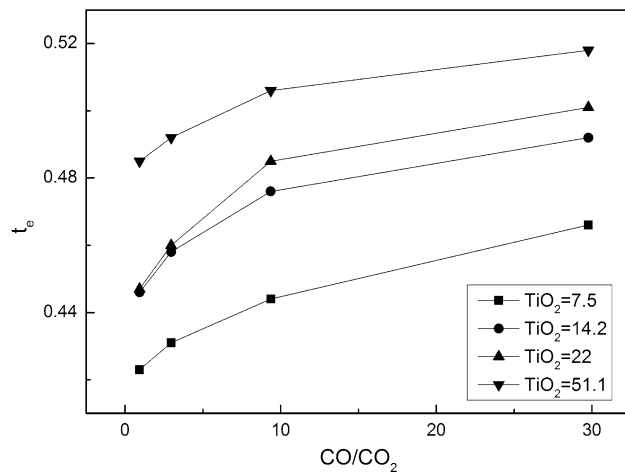


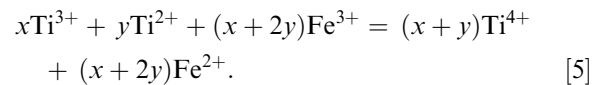
Fig. 5—The CO/CO₂ dependence of electronic transference number at 1843 K (1570 °C).

C. Ionic Conductivity

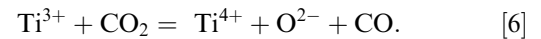
1. Influence of oxygen potential on ionic conductivity

The ionic conductivity at 1843 K (1570 °C) as a function of CO/CO₂ ratio is shown in Figure 7. It is evident from Figure 7 that the ionic conductivity of all slags increases with increasing the ratio of CO/CO₂. Tranell *et al.*^[21] studied the Ti⁴⁺-Ti³⁺ equilibria in CaO-SiO₂-TiO_x system. The total amounts of reduced titanium (Ti³⁺ and Ti²⁺) in the slags were determined by a modified version of an indirect potentiometric

redox titration method.^[22] This scheme involved dissolution of the slag in HF-HCl-H₂O solution with excess Fe³⁺ under an argon atmosphere. The reduced titanium is oxidized by the ferric ion through the following reaction:



The quantity of titanium in the Ti⁴⁺ valency state was calculated as the difference between total and reduced titanium. Since the concentration of Ti²⁺ is low in comparison with the Ti³⁺ under the present experimental conditions, all reduced titanium was approximately considered as Ti³⁺. The reaction among Ti⁴⁺, Ti³⁺, and gas is shown as follows:



From Eq. [6], it can be known that more and more Ti³⁺ will replace Ti⁴⁺ with increasing the CO/CO₂ ratio. The tendency of the Ti⁴⁺ toward covalent binding with oxygen is strong enough to stimulate the formation of highly covalent anions (TiO⁴⁻), which will lead to greatly reduced mobility compared with Ti³⁺. Therefore, the ionic conductivity of all slags increases with increasing the ratio of CO/CO₂. Figure 8 shows the ionic conductivities plotted as a function of Ti³⁺/Ti⁴⁺ ratio, values of which were taken from the work by Tranell *et al.*^[21] And the data of Figure 8 have been shown in Table III. It is seen that an increase in the fraction of Ti³⁺ increases slightly the ionic conductivity for all slags. These results can be justified by the weaker mobile ability of Ti⁴⁺ ion relative to that of Ti³⁺ ion, because of its larger electrostatic field.

2. Influence of temperature on ionic conductivity

Figure 9 shows the effect of temperature on the ionic conductivity. It can be seen that the Arrhenius law is always obeyed, and as temperature increases, ionic electrical conductivity increases, because of the decrease of viscosity and the increase of ion mobility. In addition, according to the study of Tranell *et al.*,^[21] temperature increase results in stabilization of the lower oxidation state of titanium (Ti³⁺ more stable than Ti⁴⁺), which will lead to the increase of ionic conductivity.

D. Electronic Conductivity

1. Influence of oxygen potential on electronic conductivity

Figure 10 shows the effect of the CO/CO₂ ratio on electronic conductivity at 1843 K (1570 °C). The electronic conductivity increases with increasing the ratio of CO/CO₂. Barati and Coley^[23] proposed a diffusion-assisted charge transfer model to successfully explain the electronic conductivity change of CaO-FeO-SiO₂ system. Based on this model, charge transfer can be regarded as a bimolecular reaction between Ti³⁺ and Ti⁴⁺ ions. In the first step, ions should travel to reach separation distances sufficiently short for electron

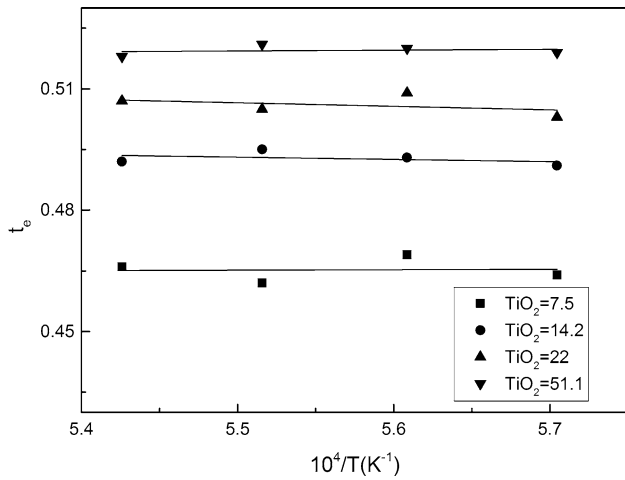


Fig. 6—The effect of temperature on the electronic transference number.

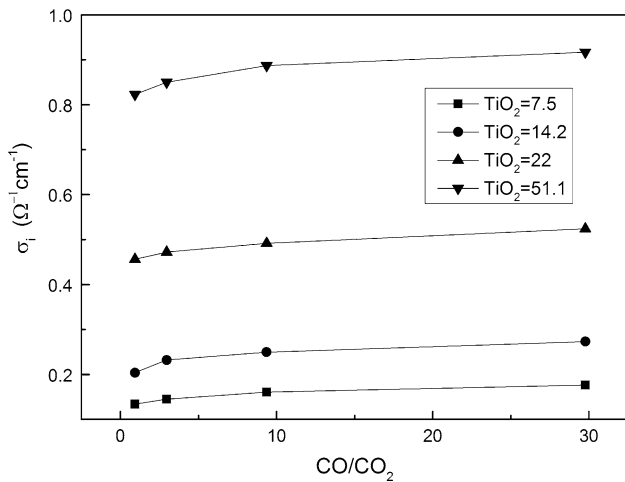


Fig. 7—The ionic conductivity at 1843 K (1570 °C) as a function of CO/CO₂ ratio.

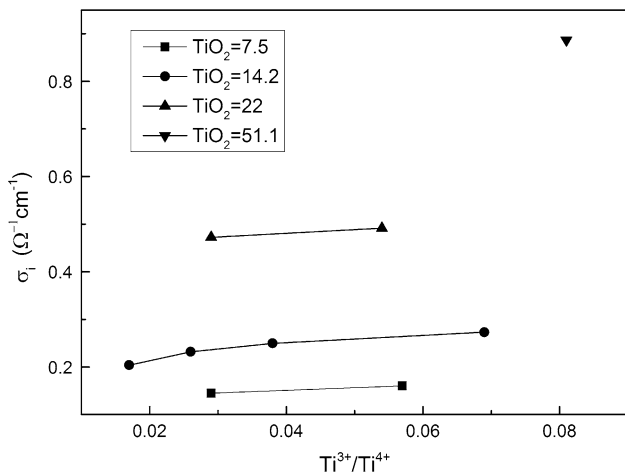


Fig. 8—The ionic conductivities of the slags plotted as a function of Ti³⁺/Ti⁴⁺ ratio.

Table III. The Change of the Ionic Conductivities ($\Omega^{-1} \text{ cm}^{-1}$) of the Slags with the Ti³⁺/Ti⁴⁺ ratio

Ti ³⁺ /Ti ⁴⁺ ratio	TiO ₂ = 7.5	TiO ₂ = 14.2	TiO ₂ = 22	TiO ₂ = 51.1
0.017	—	0.2039	—	—
0.026	—	0.2321	—	—
0.029	0.1453	—	0.4722	—
0.038	—	0.2497	—	—
0.054	—	—	0.4915	—
0.057	0.1606	—	—	—
0.069	—	0.2732	—	—
0.081	—	—	—	0.8868

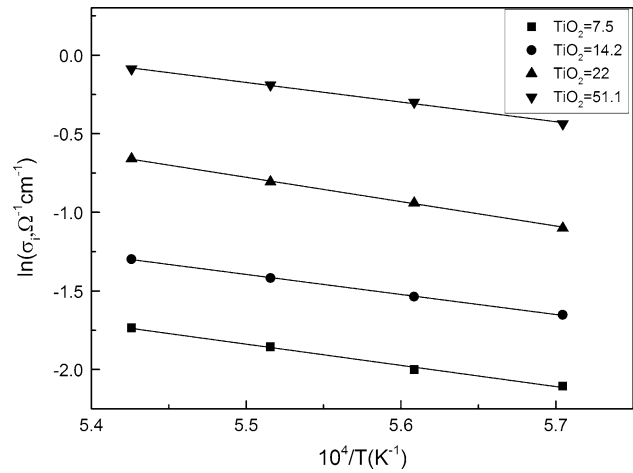


Fig. 9—The effect of temperature on the ionic conductivity at CO/CO₂ = 30.

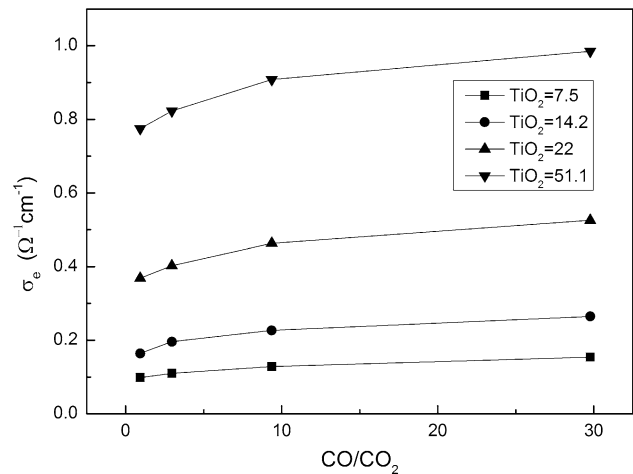


Fig. 10—The effect of the CO/CO₂ ratio on electronic conductivity at 1843 K (1570 °C).

hopping. In the next step, the electron hopping can take place. In other words, this model requires neighboring Ti³⁺ and Ti⁴⁺ ions to interact. As increasing the ratio of CO/CO₂ in a certain range, the percentage of Ti³⁺ ion will increase while that of Ti⁴⁺ ion will decrease. According to the diffusion-assisted charge transfer

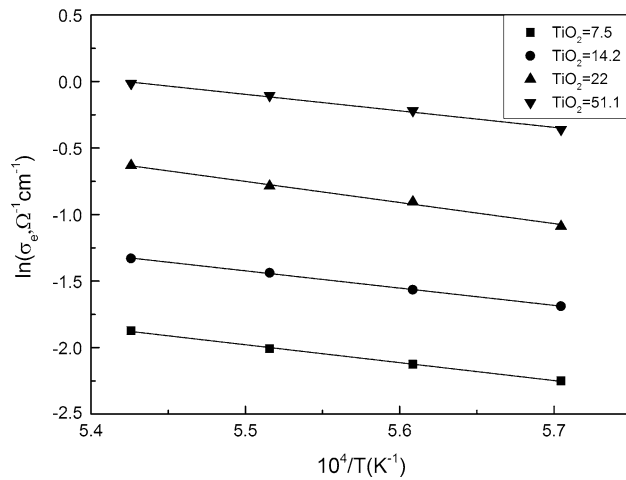


Fig. 11—The electronic conductivity as a function of temperature at $CO/CO_2 = 30$.

model, the electronic conductivity is proportional to the product of concentrations of Ti^{3+} and Ti^{4+} ions. Therefore, the electronic conductivity will increase with increasing the ratio of CO/CO_2 to a certain extent.

2. Influence of temperature on electronic conductivity

The electronic conductivity as a function of temperature is shown in Figure 11. Just like the total conductivity and ionic conductivity, the relationship between electronic conductivity and temperature also obeys the Arrhenius law, and the corresponding activation energies of the electronic conductivity are shown in Table II.

IV. CONCLUSIONS

The electrical conductivity of TiO_2 - SiO_2 - CaO slags was measured by a four-terminal technique, results of which show that the temperature dependences of ionic, electronic, and total conductivity obey the Arrhenius law. The SPC method was employed for the measurement of the electronic transference numbers, which exhibits a strong dependence on oxygen potential, while is independent of temperature. The total electrical, electronic, and ionic conductivities present similar increasing trends with increasing the ratio of CO/CO_2 , which is resulted from increasing of Ti^{3+} .

ACKNOWLEDGMENTS

Thanks are given to the financial supports from the Specialized Research Fund for the Doctoral Program of Higher Education (20130006120007) and the National Natural Science Foundation of China (51174022, 51304018 and 51474141).

REFERENCES

1. S.C. Britten and U.B. Pal: *Metall. Mater. Trans. B*, 2000, vol. 31B, pp. 733–52.
2. S. Sun and S. Jahanshahi: *Metall. Mater. Trans. B*, 2000, vol. 31B, pp. 937–43.
3. Y. Li and I.P. Ratchev: *Metall. Mater. Trans. B*, 2002, vol. 33B, pp. 624–30.
4. D. Wang, A.J. Gmitter, and D.R. Sadoway: *J. Electrochem. Soc.*, 2011, vol. 158, pp. E51–E54.
5. D.R. Sadoway: *J. Mater. Res.*, 1995, vol. 10, pp. 487–92.
6. S.L. Schiefelbein, N.A. Fried, K.G. Rhoads, and D.R. Sadoway: *Rev. Sci. Instrum.*, 1998, vol. 69, pp. 3308–13.
7. H.J. Kim, J. Paramore, A. Allanore, and D.R. Sadoway: *J. Electrochem. Soc.*, 2011, vol. 158, p. E101.
8. N.A. Fried, G.K. Rhoads, and D.R. Sadoway: *Electrochim. Acta*, 2001, vol. 46, pp. 3351–58.
9. A. Adachi and K. Ogino: *Technol. Rep. Osaka Univ.*, 1957, vol. 7 (244), pp. 121–26.
10. K. Narita, T. Onoye, T. Ishll, and K. Uemura: *ISIJ Int.*, 1975, vol. 61 (14), pp. 2943–51.
11. T. Hoster and J.P. Essen: *Arch. Eisenhütten.*, 1983, vol. 54, pp. 389–94.
12. M. Barati and K.S. Coley: *Metall. Mater. Trans. B*, 2006, vol. 37B, pp. 41–49.
13. L. Bobok, L. Bodnar, and J. Schmiedl: *Hutn. List.*, 1982, vol. 37 (6), pp. 419–24.
14. S.N. Shin, S.A. Lyamkin, R.I. Gulyaeva, and V.M. Chumarev: *Raspilvy*, 1998, vol. 5, pp. 20–24.
15. M. Kawahara, K.J. Morinaga, and T. Yanagase: *Can. Metall. Q.*, 1983, vol. 22 (2), pp. 143–47.
16. P.G. Bruce and C.A. Vincent: *J. Electroanal. Chem. Interfacial Electrochem.*, 1987, vol. 225, pp. 1–17.
17. T. Tran, S. Sun, and S. Jahanshahi: *Iron Steel Soc. AIME*, 1997, vol. 28, pp. 115–23.
18. J.H. Liu, G.H. Zhang, and K.C. Chou: *Can. Metall. Q.*, 2015, vol. 54, pp. 170–76.
19. W.R. Dickson and E.B. Dismukes: *Trans. AIME*, 1962, vol. 224, pp. 505–11.
20. E.A. Dancy and D.J. Derge: *Trans. AIME*, 1966, vol. 236, pp. 1642–48.
21. G. Tranell, O. Ostrovski, and S. Jahanshahi: *Metall. Mater. Trans. B*, 2002, vol. 33B, pp. 61–67.
22. W.P. Close and J.F. Tillman: *Glass Technol.*, 1969, vol. 10, pp. 134–46.
23. M. Barati and K.S. Coley: *Metall. Mater. Trans. B*, 2006, vol. 67B, pp. 51–60.